Saturation of superradiant light scattering from an atomic grating with a large number of atoms

Jiang Zhu,[1] Chengling Bian,[1,*] Zhibin Zhao,[1] Xing-Dong Zhao,[2,†] Lu Qin,[2] Ying-Ying Zhang,[2] Lu Zhou,[3,‡] and Guangjiong Dong[4]

[1]*School of Physics and Electronic Engineering, Hainan Normal University, Haikou 571158, China*
[2]*School of Physics, Henan Normal University, Xinxiang 453000, China*
[3]*Department of Physics, School of Physics and Electronic Science, East China Normal University, Shanghai 200241, China*
[4]*State Key Laboratory of Precision Spectroscopy, East China Normal University, Shanghai 200241, China*

(Received 22 December 2021; revised 24 April 2022; accepted 27 June 2022; published 18 July 2022)

Superradiance has drawn increasing interest, motivated by the development of quantum technology. In general, a large number of atoms are favored for inducing a strong superradiance. However, our analytical and numerical calculations of light scattering from an atomic grating longitudinally pumped by a laser show that when the atom number is small, superradiant light scattering (SLS) is induced, that is, the reflected light intensity is proportional to the square of the atom number, whereas the SLS is saturated with the increase in the atom number. In our calculation, using the coupled-wave theory, we treat the atomic grating as a dynamical photonic crystal and find rich time-dependent optical properties due to collective atomic recoil motion, which is available within research under current experimental condition. Thus, our paper could also spark an investigation of the optical features of tunable photonic crystals in the time domain.

DOI: 10.1103/PhysRevA.106.013312

I. INTRODUCTION

Superradiant light scattering (SLS) is a collectively enhanced light-scattering phenomenon which follows the well-known square law that the scattered light intensity has a square relation to the interfering atom number [1,2]. This phenomenon is analogous to Dicke's superradiance which radiates a field whose intensity becomes proportional to the square of the number of coherent radiators [3]. Now, superradiance is playing an important role in developing quantum technologies, such as quantum communication [4], quantum amplification [5], quantum memory [6–8], quantum information [9,10], quantum entanglement [11,12], as well as the optical atomic clock [13,14].

In the original Dicke model [15], superradiance is facilitated by a light-induced dipole-dipole interaction which is strong for a very short separation between atoms, therefore, a very high atom density is required. However, for the dilute atomic Bose-Einstein condensate (BEC), a series of seminal experiments in 1999 demonstrated a new mechanism that could realize the SLS [16–18]: when an elongated BEC is pumped by a laser, an optical lattice formed by lights at end-fire modes produces an atomic density grating which, in turn, increases the depth of the optical lattice, and the cooperation of the optical lattice and the atomic grating will induce a superradiance. This new mechanism is irrelevant to the quantum statistics of the atoms [19] and could also be realized in thermal gases [20]. So far, this mechanism has sparked active investigation for amplification of light and a matter wave [21], quantum phase transition [22,23], entanglement of matter waves [24], quantum imaging of atomic gases [25], as well as quantum swap of photons and matter waves [26].

An electromagnetically induced atomic grating, whose formation is a key to inducing SLS from a dilute atomic gas, has also been pursued in other fields, such as slowing light [27–29], nonlinear light diffractions [30], engineering a single photon [31], coherently enhancing backscattering [32,33], and Talbot self-imaging of an atomic gas [34,35]. However, the SLS is investigated here.

There have been intensive theoretical investigations of the superradiance of an atomic gas. One approach, first developed in coherent atom recoil lasing [36], is ray atom optics, which treats atoms as classical particles [37,38]. This classical approach is not favored for ultracold atomic gases with a rather large matter wavelength. To take account of the wave feature of ultracold atoms, the matter-wave optics approach has been developed [39–41]. This approach is successful in explaining the early stage of superradiance, matter-wave amplification, and patterns of scattered atoms. However, the relationship between the SLS and the dynamical matter-wave grating with different atom numbers has not been fully discussed.

In this paper, we treat the light scattering from an atomic grating as the Bragg reflection of light from a photonic crystal and find a saturation phenomenon of SLS with a large atom number. Previous intensive investigation of atomic photonic crystals [42–45] has not linked the Bragg reflection to SLS. Now, our analytical and numerical solutions show that when the atom number is low, a SLS could be induced, that is, the reflectance of the atomic Bragg grating is proportional to the square of the atom number. However, when the atom number increases, the SLS is saturated, in other words, the square law

*bcl.200801@163.com
†phyzhxd@gmail.com
‡lzhou@phy.ecnu.edu.cn

is violated. This surprising result may shed light on understanding the scaling law for the cooperative optical effect of atomic gases. Also, our paper could inspire investigation of tunable photonic crystals within the time domain.

We organize this paper as follows. The physical model of the interaction between light and an atomic grating is presented in Sec. II. An analytical solution of the reflectance of the atomic grating is given in Sec. III, and saturation of the SLS is discussed. In Sec. IV, we analyze the light field by the modified coupled-wave theory (MCWT) [46], and then numerically calculate the reflectance of the atomic grating with different atom numbers and momentum distributions. A comparison between the numerical and the analytical solutions is given. In Sec. V, we discuss the validity of our one-dimensional semiclassical model. We conclude in Sec. VI by briefly summarizing our results and providing an outlook.

II. PHYSICAL MODEL

We start our analysis from the equation for the wave-function $\Psi(\boldsymbol{r},t)$ of a two-level atomic BEC driven by a far-off resonant optical field under the Gross-Pitaevskii mean-field approximation [47],

$$i\hbar\frac{\partial}{\partial t}\Psi(\boldsymbol{r},t)=\left[-\frac{\hbar^2\nabla^2}{2M}+\frac{|\boldsymbol{d}\cdot\boldsymbol{E}(\boldsymbol{r},t)|^2}{\hbar\Delta}\right]\Psi(\boldsymbol{r},t)+[V_{\rm trap}(\boldsymbol{r})+g|\Psi(\boldsymbol{r},t)|^2]\Psi(\boldsymbol{r},t),\quad(1)$$

where $\Psi(\boldsymbol{r},t)$ is subjected to the normalization condition: $\int_{-\infty}^{+\infty}d\boldsymbol{r}|\Psi(\boldsymbol{r},t)|^2=1$. $V_{\rm trap}(\boldsymbol{r})$ is an extra trapping potential confining the BEC. g is the effective s-wave atom-atom interaction strength. $\Delta=\omega_{\rm L}-\omega_{\rm a}$ is the detuning of the laser frequency $\omega_{\rm L}$ from the atomic resonance frequency $\omega_{\rm a}$. $\boldsymbol{d}$ is the dipole matrix element between the ground and the excited states. $\boldsymbol{E}(\boldsymbol{r},t)$ describes the slowly varying amplitude of the optical field interacting with the condensate which satisfies the Helmholtz equation [48],

$$\nabla^2\boldsymbol{E}(\boldsymbol{r},t)+k_{\rm L}^2n^2(\boldsymbol{r},t)\boldsymbol{E}(\boldsymbol{r},t)=0,\quad(2)$$

where $k_{\rm L}=\omega_{\rm L}/c$ is the wave number of the optical field in vacuum. The refractive index $n(\boldsymbol{r},t)$ in Eq. (2) of the condensate is given by [49]

$$n(\boldsymbol{r},t)=\sqrt{1+\chi},\quad(3)$$

where $\chi=-d^2N/(\epsilon_0\hbar\Delta)|\Psi(\boldsymbol{r},t)|^2$ is the susceptibility of the BEC, N is the atom number, and ϵ_0 is the vacuum permittivity.

In order to study the reflection of light by an atomic grating, we first reduce the atom-field system to a quasi-one-dimensional (1D) one. We assume a cigar-shaped BEC with length L and effective cross-section area Z whose transverse freedom is frozen by a tightly bounded trapping potential $V_{\rm trap}(\boldsymbol{r})=V_{\rm trap}(y,z)$, whereas $V_{\rm trap}(x)=0$. Moreover, we consider the transverse width of the optical fields is much larger than $\sqrt{Z}$ such that the transverse dispersion of the optical field and the matter wave could be neglected in our further analysis. Furthermore, the optical field is assumed to be linearly polarized along the z direction. Then the BEC wave function and the optical field could be expressed as $\Psi(\boldsymbol{r},t)=\psi(x,t)/\sqrt{Z}$ and $\boldsymbol{E}(\boldsymbol{r},t)=E(x,t)\hat{e}_z$. To focus on the interaction between atoms and light, the collisions between atoms are neglected which can be realized by means of the Feshbach resonance technique [50]. Consequently, the coupled Eqs. (1) and (2) could be reduced to

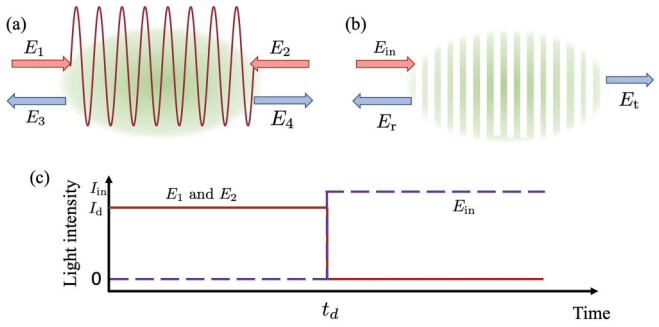

FIG. 1. (a) Two counterpropagating lights E_1 and E_2 are used to produce an atomic density grating in a BEC. Outside the condensate, E_3 and E_4 are scattered optical fields. (b) Bragg reflection of the incident light $E_{\rm in}$ from the prepared atomic density grating. $E_{\rm r}$ ($E_{\rm t}$) is the reflected (transmitted) light. (c) The time-sequence diagram of light.

$$i\hbar\frac{\partial}{\partial t}\psi(x,t)=\left[-\frac{\hbar^2}{2M}\frac{\partial^2}{\partial x^2}+\frac{d^2}{\hbar\Delta}|E(x,t)|^2\right]\psi(x,t),\quad(4)$$

$$\frac{\partial^2}{\partial x^2}E(x,t)+k_{\rm L}^2n^2E(x,t)=0.\quad(5)$$

In the 1D Helmholtz equation (5), the refractive index becomes

$$n=\sqrt{1+\beta N|\psi(x,t)|^2},\quad(6)$$

where $\beta=-d^2/(Z\epsilon_0\hbar\Delta)$.

The physical mechanism of the SLS in experiment of a cigar-shaped BEC end pumped by a single light field is that an atomic grating in the BEC accumulates continuously due to seeding by spontaneous photon emission in the direction opposite to the pump beam. However, here we do not directly study the atomic grating generated by spontaneous emission in the experiment but use the atomic grating prepared by an optical lattice as a substitute. The reason for this substitution is that the preparation and the reflectance of the atomic grating are easy to manipulate and calculate. It should be noted that this substitution does not affect our study of the physical mechanism of the SLS.

For creating an atomic grating, we are concerned with the cigar-shaped BEC longitudinally irradiated by two counterpropagating coherent optical fields E_1 and E_2 for a duration $t_{\rm d}$ as shown in Fig. 1(a), the atomic grating is obtained by Bragg diffraction of the condensate in the optical lattice formed by E_1 and E_2. When E_1 and E_2 are switched off, a third light field $E_{\rm in}$ is incident on the created atomic grating as shown in Fig. 1(b). Then, the reflectance R can be calculated by

$$R=\left|\frac{E(0,t)-E_{\rm in}}{E_{\rm in}}\right|^2.\quad(7)$$

III. ANALYTICAL CALCULATION OF THE REFLECTANCE

In view of the fact that an atomic grating is similar to a photonic crystal, the standard coupled-wave theory (SCWT) [46] can be used to study the optical properties of the atomic grating. In order to describe the main optical properties, the wave function of the BEC at time $t \geqslant t_{\rm d}$ can be expanded onto plane waves which correspond to different Bragg diffraction orders as

$$\psi(x,\tau) = \frac{1}{\sqrt{L}} \sum_m c_m(\tau) \exp(2im\bar{k}x), \tag{8}$$

where $\tau = t - t_{\rm d}$, $\bar{k} = k_{\rm L} n_0$ is the effective wave number of the optical field in the atomic grating, $n_0 = \sqrt{1+\beta N/L}$ is defined as the average refractive index of the atomic grating. For $\tau \geqslant 0$, we assume the incident light $E_{\rm in}$ is so weak that the wave function (8) evolves almost freely, i.e., the momentum components of the atomic grating evolve as $c_m(\tau) = c_m(0)\exp(-4im^2\bar{\omega}_{\rm r}\tau)$, where $\bar{\omega}_{\rm r} = \hbar\bar{k}^2/(2M)$ is the effective recoil frequency and $c_m(0)$ is determined by the duration $t_{\rm d}$. Substituting Eq. (8) into Eq. (6), the square of refractive index of the atomic grating can be expressed as

$$n^2(x) = n_0^2 + \beta N \sum_{l(l\neq 0)} b_l \exp(2il\bar{k}x), \tag{9}$$

where $b_l = \sum_m c_m^*(\tau)c_{m+l}(\tau)/L$. Equation (9) shows the periodicity of the refractive index of the atomic grating. Expressing the solution of Eq. (5) in the form of a superposition of two counterpropagating waves as

$$E(x) = A^+(x)\exp(i\bar{k}x) + A^-(x)\exp(-i\bar{k}x), \tag{10}$$

and substituting Eqs. (9) and (10) into Eq. (5), we obtain the approximate set of coupled equations for the forward and backward wave amplitudes A^+ and A^- by the SCWT,

$$\frac{d}{dx}A^{\pm}(x) = \pm i\eta b_{\pm 1}A^{\mp}(x), \tag{11}$$

where $\eta = k_{\rm L}^2\beta N/2$. The general solution of Eq. (11) is

$$\begin{aligned} A^+(x) &= C_1\exp(-\eta|b_1|x) + C_2\exp(\eta|b_1|x),\\ A^-(x) &= i[C_1\exp(-\eta|b_1|x) - C_2\exp(\eta|b_1|x)]\exp(-i\theta), \end{aligned} \tag{12}$$

where $b_1 = |b_1|\exp(i\theta)$, $b_{-1} = b_1^* = |b_1|\exp(-i\theta)$. Considering the boundary conditions $A^+(0) = E_{\rm in}$ and $A^-(L) = 0$, we obtain the following expression for the first-order Bragg reflectance of the atomic grating:

$$R = \tanh^2(\eta|b_1|L) = \tanh^2\left(\gamma N\left|\sum_m c_m^*(\tau)c_{m+1}(\tau)\right|\right), \tag{13}$$

where $\gamma = k_{\rm L}\beta/(2n_0)$. Equation (13) shows that the reflectance is independent of the length of the atomic grating. We further note that $\gamma \sim 10^{-7}$ under the current experimental conditions which are used in Part IV for the numerical simulation. Therefore, when the atom number is small $R \propto N^2$, which means that there is SLS from the atomic grating. However, the superradiance is saturated when the atom number is large.

The results of reflectance for the atomic grating above is reasonable because physically, reflectance cannot increase with the atom number unlimitedly due to the constraint $R \leqslant 1$. Consequently, the N^2 law is an approximate of Eq. (13) when N is small.

If $|E_1| = |E_2|$ and the atoms of the grating are almost all distributed in the momentum components with $m = 0, \pm 1$, the summation in Eq. (13) can be simplified to $c_{-1}^*(\tau)c_0(\tau) + c_0^*(\tau)c_1(\tau)$. In view of the symmetry of the atomic grating, we let $c_{\pm 1}(0) = |c_1(0)|\exp(i\theta_{\pm 1})$ and $c_0(0) = |c_0(0)|\exp(i\theta_0)$, we obtain

$$\left|\sum_m c_m^*(\tau)c_{m+1}(\tau)\right| \approx |c_0(0)||c_1(0)|\sqrt{2+2\cos(8\bar{\omega}_{\rm r}\tau+\Theta)}, \tag{14}$$

where $\Theta = 2\theta_0 - \theta_1 - \theta_{-1}$ is a constant phase. Equation (14) together with Eq. (13) shows that the reflectance R oscillates periodically with time. When the atom number is small, $R \propto \cos(8\bar{\omega}_{\rm r}\tau + \Theta)$ and the oscillation period of the reflectance is $2\pi/(8\bar{\omega}_{\rm r})$.

IV. NUMERICAL SIMULATION

A. Relationship between the reflectance and the atom number

For the numerical investigation of light reflection by the atomic grating, using the MCWT, we first substitute in Eq. (5) the solution for $E(x)$ in the form of counterpropagating waves with variable amplitudes A^+ and A^-,

$$E(x) = \frac{1}{\sqrt{n(x)}}[A^+(x)e^{i\varphi(x)} + A^-(x)e^{-i\varphi(x)}], \tag{15}$$

where $\varphi(x) \equiv k_L\int_0^x n(u)du$. The amplitudes A^+ and A^- of the forward and backward propagating waves in the condensate satisfy the equations,

$$\frac{d}{dx}A^{\pm}(x) = S^{\mp}(x)A^{\mp}(x), \tag{16}$$

where $S^{\pm}(x) = 1/(2n)(dn/dx)\exp[\pm 2i\varphi(x)]$. It is important to note that $E(x)$ is redefined in Eq. (15) for the purposes of numerical modeling and, thus, differs from Eq. (10). This also leads to a change in the equation for the amplitudes, i.e., Eq. (16) replaces Eq. (11). Moreover, the derivation of Eq. (16) from Eq. (5) involved no approximation.

In the numerical simulation, we assume the BEC is formed by Rb^{87} atoms with a Gaussian initial wave function,

$$\Psi(\boldsymbol{r},0) = \sqrt{\frac{1}{Z\sqrt{\pi}w_x}}\exp\left[-\frac{(x-L/2)^2}{2w_x^2}\right], \tag{17}$$

where $Z \equiv \pi w_\perp^2$, the parameters $w_x = 50\ \mu$m and $w_\perp = 10\ \mu$m. The transition between $5^2S_{1/2}$ and $5^2P_{3/2}$ is used. We assume the wave-number $k_{\rm L} = 8.055\times 10^6\ {\rm m}^{-1}$ and the detuning $\Delta = 2\pi\times(-1.5)$ GHz so that the parameter $\beta = 7.74\times 10^{-14}$ m. For creating the atomic grating, the light intensity of E_1 and E_2 is $I_{\rm d} = 3\ {\rm mW/cm^2}$, the duration $t_{\rm d} = 10\ \mu$s. The finite difference method and operator splitting method are used to solve Eqs. (4), (15), and (16).

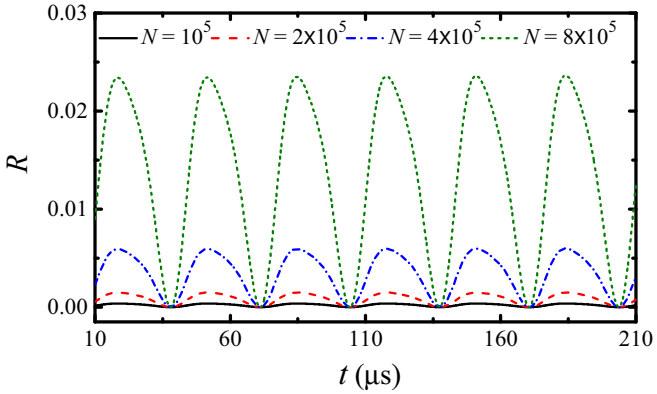

FIG. 2. Time evolution of reflectance R for different atom numbers N in the case that $I_{\rm in} = 0.1\ {\rm mW/cm^2}$.

Figure 2 shows the reflectance of the atomic density grating for the incident light intensity $I_{\rm in} = 0.1\ {\rm mW/cm^2}$, which is much less than $I_{\rm d}$. The reason for using weak light incidence here is that the atomic grating is hardly changed by the incident light field when the reflectance is detected within the considered timescale, which will be discussed in detail in part C of this Section.

As shown in Fig. 2, the reflectance varies periodically with time as predicted in Eq. (14) due to the atom recoil motion in the atomic grating and the period is independent from the atom number. More interestingly, the reflectance peak increases greatly when the atom number is doubled. Thus, in Fig. 3 we study the relation of the first reflectance peak $R_{\rm P}$ to the atom number N (black dots). We find that the points for the reflectance peak versus the atom number is very well fitted by the function,

$$R_{\rm P} = \tanh^2(\xi N/10^5), \tag{18}$$

with $\xi = 1.93 \times 10^{-2}$ as shown by the red solid line in Fig. 3, which is approximately proportional to N^2 when the atom number is small ($N \lesssim 2 \times 10^6$), implying SLS. However, when the atom number increases further, the SLS is gradually saturated, which is more clearly shown in the inset of Fig. 3

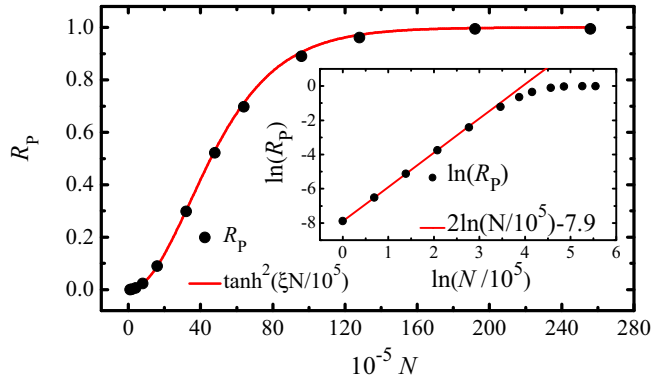

FIG. 3. The relation of the first reflectance peak $R_{\rm P}$ in Fig. 2 to the atom number N (black dots). The red solid line is a fitting line. The inset is a logarithmic plot of the reflectance peak to the atom number (black dots). The slope of the red line for comparison is 2.

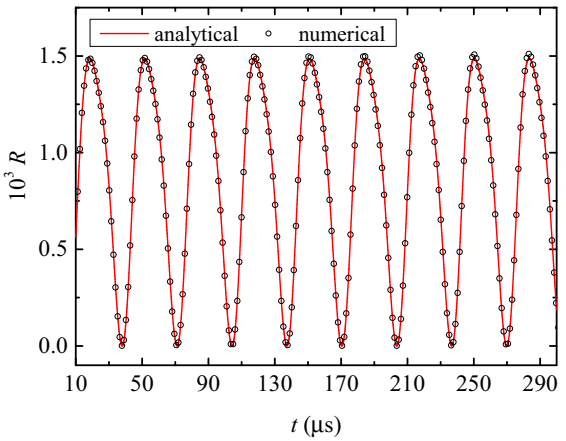

FIG. 4. Analytical (red solid line) and numerical (black circle) time evolution of the reflectance R of the atomic grating with atom number $N = 2 \times 10^5$ in the case that $I_{\rm in} = 0.1\ {\rm mW/cm^2}$.

that in the double logarithmic coordinate, the slope of the relationship between $R_{\rm P}$ and N gradually decreases from 2 to 0 (black dots). It should be noted that the form of Eq. (18) is the same as that of Eq. (13), and the parameter ξ in Eq. (18) is consistent with the value that can be obtained by directly applying Eq. (13).

Figure 4 shows that the analytical oscillation curve of the reflectance (red solid line) calculated by Eq. (13) is in good agreement with the numerical one (black circle). Before analytically calculating the reflectance, the generation of the atomic grating is performed by numerical simulation. Then the red solid line in Fig. 4 is obtained by substituting the momentum distribution of the atomic grating into Eq. (13). The red solid line and the black circles in Fig. 4 deviated slightly with the evolution of time. It is mainly because in the numerical simulation, the momentum distribution of the atomic gas has a slight change over time due to the weak incident light, whereas the analytical reflectance is obtained under the condition of free evolution of the atomic gas.

B. Relationship between the reflectance and the atomic momentum distribution

The reflectance of the atomic grating depends not only on the atom number, but also on the momentum distribution $\phi(p,t) = \int_{-\infty}^{+\infty} \psi(x,t)\exp(ipt/\hbar)dx/\sqrt{2\pi}$ of the atomic grating which is controlled by the duration $t_{\rm d}$ of E_1 and E_2. Therefore, we study the relation of the reflectance peak and atomic momentum components to the duration $t_{\rm d}$, respectively, in Figs. 5(a) and 5(b) under the condition that $N = 2 \times 10^5$, $I_{\rm d} = 3\ {\rm mW/cm^2}$, and $I_{\rm in} = 0.1\ {\rm mW/cm^2}$. Because the momentum distribution of the atomic gas is symmetrical and concentrated at $\pm 2m\hbar\bar{k}$, only nonnegative momentum components with $m = 0$–2 are given in Fig. 5(b). This figure implies that in the considered duration ($t_{\rm d} < 80\ \mu{\rm s}$), the atoms are mainly distributed in the momentum components with $m = 0, \pm 1$. Moreover, Fig. 5 shows that the reflectance is very small when the self-imaging of the matter wave [51] appears at $t_{\rm d} \approx 40,\ 80\ \mu{\rm s}$ because almost all atoms are distributed on the zero momentum component and there is almost no atomic

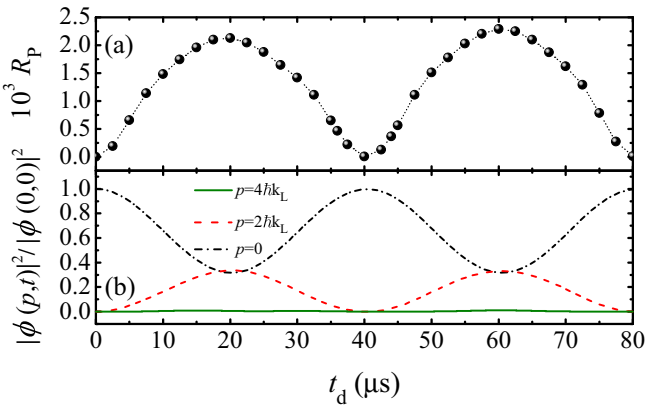

FIG. 5. (a) The relation of the first reflectance peak to the duration t_d. (b) The relation of the momentum distribution of the atomic gas to the duration t_d, only three momentum components 0, $2\hbar\bar{k}$, and $4\hbar\bar{k}$ are shown.

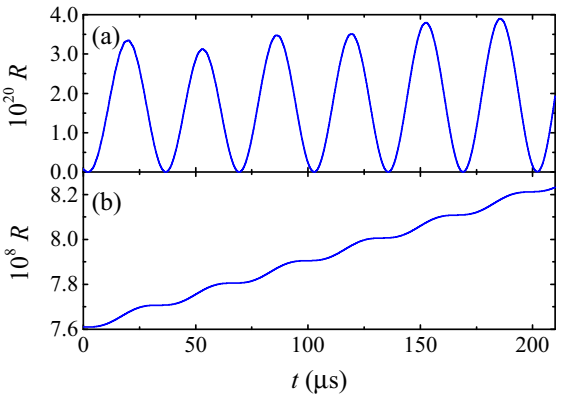

FIG. 6. Time evolution of the reflectance of an atomic gas with 8×10^5 atoms and a Gaussian initial distribution end pumped by a single light field with an intensity of $I_{in} = 0.1$ mW/cm^2. (a) No seeding by spontaneous photon emission; (b) seeding the dynamics by spontaneous photon emission.

grating in the BEC. However, when the atom number of the momentum components with $m = 0, \pm 1$ is almost equal ($t_d \approx 20,\ 60\ \mu$s), the matter-wave interference is strong, and the reflectance of the atomic grating reaches the maximum. Here, the incident light together with the momentum component $m\hbar\bar{k}$ of the atomic gas, the momentum component $(m+1)\hbar\bar{k}$, and the reflected light from the atomic grating, respectively, correspond to the excited state, the ground state, and the cooperative radiation of the molecule system in Dicke's superradiance model where the largest spontaneous radiation rate will be achieved when the number of molecules in the excited state is equal to that in the ground state.

C. Discussion on the atomic grating

In order to show the importance of an atomic grating for efficient light scattering, we study the light reflection of a BEC with the Gaussian wave function given by Eq. (17) end pumped by a single light field with an intensity of $I_{in} = 0.1$ mW/cm^2. First, as a theoretical idealization, under the assumption that there is no seeding by spontaneous photon emission as shown in Fig. 6(a), the reflectance of the Gaussian atomic gas is negligible. Second, as a numerical simulation of the experiment of SLS caused by spontaneous emission, we seed the dynamics by making a nonzero first-order momentum component equal to $\Psi(\boldsymbol{r}, 0)/\sqrt{N}$, corresponding to a single delocalized atom in the first side mode [2]. As shown in Fig. 6(b), spontaneous photon emission greatly improves the reflectance due to the accumulation of an atomic grating in the dilute atomic gas. However, within the timescale $t_r = 2\pi/\bar{\omega}_r \sim 10^{-4}$ s, the reflectance in Fig. 6(b) is much smaller than that of the atomic grating built by the optical lattice as shown in Fig. 2. This is because that I_{in} is so weak that the corresponding single-photon scattering rate is $R_{sc} \sim 3\ \mathrm{s}^{-1}$, which is much smaller than the recoil frequency $\bar{\omega}_r$. The single-photon scattering rate can be calculated by [2]

$$R_{sc} = \left(\frac{\Gamma}{2}\right)\frac{I_{in}/I_s}{1 + 4(\Delta/\Gamma)^2 + (I_{in}/I_s)}, \tag{19}$$

where Γ is the natural decay rate and I_s is the saturation intensity of the optical transition. For the transition used in the present paper, $\Gamma = 2\pi \times 6.07$ MHz, and $I_s = 2.504$ mW/cm^2. Such a small R_{sc} means that the timescale for that the SLS seeded by the spontaneous emission can significantly affect the atom momentum distribution is much longer than the timescale we considered ($\sim t_r$). Consequently, we neglect the spontaneous photon emission in the calculation of Figs. 2–5. By the same token, the SLS seeded by the spontaneous photon emission is neglected in the process of creating the atomic grating by the optical lattice because the timescale it can significantly affect atom momentum distribution is much longer than the duration t_d.

V. VALIDITY OF THE SEMICLASSICAL MODEL

The relationship between the present paper and [2,41] can be established by calculating the experimental and theoretical results in Ref. [2] via numerical simulation on Eqs. (4), (15), and (16) with the seeding method of driving the SLS as mentioned in Part IV C. Figure 7 shows that the backscattered photon flux of our calculations with the experimental parameters in Ref. [2] are consistent with Fig. 4 in Ref. [2] regarding the first reflected pulse signal which is supported by the experimental data. In this numerical simulation, the initial wave function of the BEC containing 1.36×10^6 Rb^{87} atoms is also Eq. (17) where the parameters $w_x = 100$ and $w_\perp = 10\ \mu$m. The transition between $5^2S_{1/2}$ and $5^2P_{1/2}$ is used. We assume the wave-number $k_L = 7.90 \times 10^6$ m^{-1} and the detuning $\Delta = 2\pi \times (-2.6)$ GHz so that the parameter $\beta = 6.72 \times 10^{-14}$ m. For Fig. 7, Eq. (19) is used, where $\Gamma = 2\pi \times 5.75$ MHz, and $I_s = 4.4876$ mW/cm^2.

Moreover, as shown in Fig. 8, a numerical study on the atom number dependence of the peak value of the first superradiant pulse for the experimental situation of Ref. [2] would give a result similar to that depicted in Fig. 3, however, without an initially prepared atomic grating. The superradiant pulse amplitude has quadratic dependence on atom number N when N is relatively small, which is consistent with that

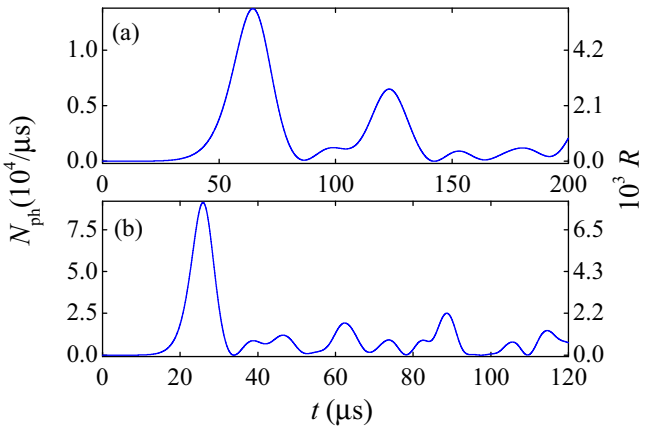

FIG. 7. Simulation of the time trace of the backscattered photon flux (measured by the left vertical axis) with the experimental parameters in Ref. [2] for different single-particle scattering rates R_{sc}. The right vertical axis shows the corresponding reflectance. (a) $R_{sc} = 0.447 \times 10^3\ s^{-1}$, i.e., $I_{in} = 90.8\ mW/cm^2$; (b) $R_{sc} = 2.15 \times 10^3\ s^{-1}$, i.e., $I_{in} = 436.85\ mW/cm^2$.

reported in Ref. [2], and will be saturated with the increase in N.

Indeed, the one-dimensional semiclassical model we used has similar defects to the one-dimensional Maxwell-Schödinger equation used in Refs. [2,41], e.g., the decoherence mechanism in the system and the different speeds of the dynamics for different radial layers of the BEC caused by inhomogeneous transverse density distribution are not considered, which will increase the difference between the theoretical calculation and the experimental data in the long-time run. However, within the timescale concerned in this paper ($\sim t_r$), especially within the time of the first reflected pulse, these defects will not have a strong affection on the main results in this paper as supported by Fig. 7.

It should also be noted that SLS seeded by spontaneous emission will take effect in the long-time run, especially by considering that spontaneous emission takes place occasionally, thus, making Fig. 2 less regular and deforming Fig. 5 at times where reflectance is currently predicted to be close to zero. Such random processes cannot be properly accounted within the present theoretical framework.

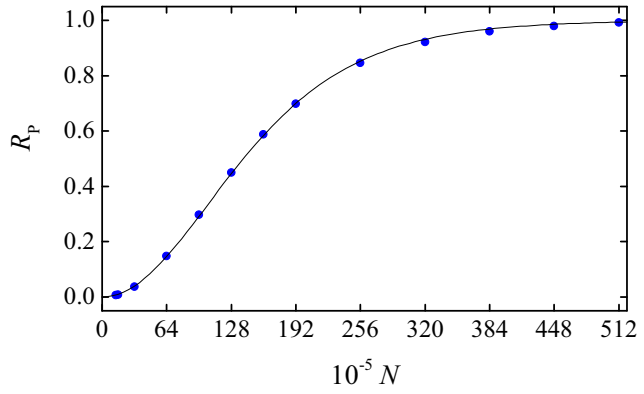

FIG. 8. The relation of the first reflectance peak R_P to the atom number N of the experimental situation of Ref. [2] with the parameters of Fig. 7(a) (blue dots). A fitting function $R_P = \tanh^2(\zeta N/10^5)$, where $\zeta = 6.3 \times 10^{-3}$ is plotted by the solid line.

VI. CONCLUSION AND OUTLOOK

To summarize, we have studied the SLS from an atomic grating longitudinally pumped by a laser and treated the atomic grating as a photonic crystal. Both the analytical and the numerical calculations show that the intensity peak of the reflected light increases with a quadric hyperbolic tangent function of the atom number. When the atom number is small, the intensity peak is quadratically proportional to the atom number, showing SLS. However, when the atom number increases further, this square law is violated, that is, the SLS is saturated. Moreover, this light scattering is controllable by manipulating the momentum components of the atomic grating. Our theoretical results are obtained under current experimental conditions.

Previously, suppression of superradiance was found in collective cavity cooling of molecules when the molecule number is large due to defect of molecule distribution [52–54]. Now, we demonstrate a mechanism for the suppression of superradiance for an atomic gas with a large number of atoms, resulting from that the SLS will be saturated with the increase in the atom number. This saturation is due to the fact that superradiant light intensity cannot be greater than the pumping light intensity. Thus, our results are independent of the model and would cast light on understanding the scaling laws in cooperative optical effect of atomic or molecular gases. For example, we could explore whether collective atom recoil lasing could violate the scaling law of $N^{4/3}$ [55] when the atom number is very large.

Our analysis also shows that atomic gratings have rich time-dependent optical properties due to the atom recoil motion. According to our paper, the oscillation of the reflected light intensity as implied by Eq. (14), could be used in precision measurement experiments with matter waves, and an approach to controlling the reflectance of light from the atomic grating by manipulating the duration t_d may be proposed based on Fig. 5. Our paper could also spark the investigation of tunable solid photonic crystals in the time domain.

ACKNOWLEDGMENTS

This work was supported by the Major Science and Technology Program of Hainan Province of China under Grant No. ZDKJ2019005, the National Natural Science Foundation of China under Grants No. 11374003, No. 11604086, No. 11764012, No. 12074120, No. 61774024, No. 61864002, and No. 61964007, the Young Talents Science and Technology Innovation Project of Hainan Association for Science and Technology under Grant No. QCXM201810, and the Natural Science Foundation of Shanghai.

[1] H. Uys and P. Meystre, Cooperative scattering of light and atoms in ultracold atomic gases, Laser Phys. Lett. **5**, 487 (2008).

[2] J. H. Müller, D. Witthaut, R. le Targat, J. J. Arlt, E. S. Polzik, and A. J. Hilliard, Semi-classical dynamics of superradiant Rayleigh scattering in a Bose-Einstein condensate, J. Mod. Opt. **63**, 1886 (2016).

[3] M. Gross and S. Haroche, Superradiance: An essay on the theory of collective spontaneous emission, Phys. Rep. **93**, 301 (1982).

[4] M. O. Scully and A. A. Svidzinsky, The Super of Superradiance, Science **325**, 1510 (2009).

[5] A. A. Svidzinsky, L. Yuan, and M. O. Scully, Quantum Amplification by Superradiant Emission of Radiation, Phys. Rev. X **3**, 041001 (2013).

[6] A. T. Black, J. K. Thompson, and V. Vuletić, On-Demand Superradiant Conversion of Atomic Spin Gratings into Single Photons with High Efficiency, Phys. Rev. Lett. **95**, 133601 (2005).

[7] M. S. Mendes, P. L. Saldanha, J. W. R. Tabosa, and D. Felinto, Dynamics of the reading process of a quantum memory, New J. Phys. **15**, 075030 (2013).

[8] B. P. Marsh, Y. Guo, R. M. Kroeze, S. Gopalakrishnan, S. Ganguli, J. Keeling, and B. L. Lev, Enhancing Associative Memory Recall and Storage Capacity Using Confocal Cavity QED, Phys. Rev. X **11**, 021048 (2021).

[9] D. D. Yavuz, Superradiance as a source of collective decoherence in quantum computers, J. Opt. Soc. Am. B **31**, 2665 (2014).

[10] F. Dinc and A. M. Brańczyk, Non-Markovian superradiance in a linear chain of up to 100 qubits, Phys. Rev. Research **1**, 032042(R) (2019).

[11] Y. N. Chen, T. Brandes, C. M. Li, and D. S. Chuu, Shot-noise spectrum of superradiant entangled excitons, Phys. Rev. B **69**, 245323 (2004).

[12] M. Aparicio Alcalde, A. H. Cardenas, N. F. Svaiter, and V. B. Bezerra, Entangled states and superradiant phase transitions, Phys. Rev. A **81**, 032335 (2010).

[13] M. A. Norcia, M. N. Winchester, J. R. K. Cline, and J. K. Thompson, Superradiance on the millihertz linewidth strontium clock transition, Sci. Adv. **2**, e1601231 (2016).

[14] D. Pan, B. Arora, Y. Yu, B. K. Sahoo, and J. Chen, Optical-lattice-based Cs active clock with a continual superradiant lasing signal, Phys. Rev. A **102**, 041101(R) (2020).

[15] R. H. Dicke, Coherence in Spontaneous Radiation Processes, Phys. Rev. **93**, 99 (1954).

[16] S. Inouye, A. P. Chikkatur, D. M. Stamper-Kurn, J. Stenger, D. E. Pritchard, and W. Ketterle, Superradiant Rayleigh Scattering from a Bose-Einstein Condensate, Science **285**, 571 (1999).

[17] S. Inouye, T. Pfau, S. Gupta, A. P. Chikkatur, A. Görlitz, D. E. Pritchard, and W. Ketterle, Phase-coherent amplification of atomic matter waves, Nature (London) **402**, 641 (1999).

[18] M. Kozuma, Y. Suzuki, Y. Torii, T. Sugiura, T. Kuga, E. W. Hagley, and L. Deng, Phase-Coherent Amplification of Matter Waves, Science **286**, 2309 (1999).

[19] P. Wang, L. Deng, E. W. Hagley, Z. Fu, S. Chai, and J. Zhang, Observation of Collective Atomic Recoil Motion in a Degenerate Fermion Gas, Phys. Rev. Lett. **106**, 210401 (2011).

[20] Y. Yoshikawa, Y. Torii, and T. Kuga, Superradiant Light Scattering from Thermal Atomic Vapors, Phys. Rev. Lett. **94**, 083602 (2005).

[21] S. Inouye, R. F. Löw, S. Gupta, T. Pfau, A. Görlitz, T. L. Gustavson, D. E. Pritchard, and W. Ketterle, Amplification of Light and Atoms in a Bose-Einstein Condensate, Phys. Rev. Lett. **85**, 4225 (2000).

[22] K. Baumann, C. Guerlin, F. Brennecke, and T. Esslinger, Dicke quantum phase transition with a superfluid gas in an optical cavity, Nature (London) **464**, 1301 (2010).

[23] X. Zhang, Y. Chen, Z. Wu, J. Wang, J. Fan, S. Deng, and H. Wu, Observation of a superradiant quantum phase transition in an intracavity degenerate Fermi gas, Science **373**, 1359 (2021).

[24] L. F. Buchmann, G. M. Nikolopoulos, O. Zobay, and P. Lambropoulos, Correlated directional atomic clouds via four-heterowave mixing, Phys. Rev. A **81**, 031606(R) (2010).

[25] L. E. Sadler, J. M. Higbie, S. R. Leslie, M. Vengalattore, and D. M. Stamper-Kurn, Coherence-Enhanced Imaging of a Degenerate Bose-Einstein Gas, Phys. Rev. Lett. **98**, 110401 (2007).

[26] M. E. Taşgın, M. Ö. Oktel, L. You, and Ö. E. Müstecaplıoğlu, Quantum correlated light pulses from sequential superradiance of a condensate, Phys. Rev. A **79**, 053603 (2009).

[27] K. R. Hansen and K. Mølmer, Stationary light pulses in ultracold atomic gases, Phys. Rev. A **75**, 065804 (2007).

[28] I. Iakoupov, J. R. Ott, D. E. Chang, and A. S. Sørensen, Dispersion relations for stationary light in one-dimensional atomic ensembles, Phys. Rev. A **94**, 053824 (2016).

[29] J. L. Everett, D. B. Higginbottom, G. T. Campbell, P. Koy Lam, and B. C. Buchler, Stationary Light in Atomic Media, Adv. Quantum Technol. **2**, 1800100 (2019).

[30] C. Hang, W. Li, and G. Huang, Nonlinear light diffraction by electromagnetically induced gratings with $\mathcal{PT}$ symmetry in a Rydberg atomic gas, Phys. Rev. A **100**, 043807 (2019).

[31] J. Wen, Y. Zhai, S. Du, and M. Xiao, Engineering biphoton wave packets with an electromagnetically induced grating, Phys. Rev. A **82**, 043814 (2010).

[32] Y. V. Rostovtsev, Z. Sariyanni, and M. O. Scully, Electromagnetically Induced Coherent Backscattering, Phys. Rev. Lett. **97**, 113001 (2006).

[33] H. L. Sørensen, J.-B. Béguin, K. W. Kluge, I. Iakoupov, A. S. Sørensen, J. H. Müller, E. S. Polzik, and J. Appel, Coherent Backscattering of Light Off One-Dimensional Atomic Strings, Phys. Rev. Lett. **117**, 133604 (2016).

[34] J. Wen, S. Du, H. Chen, and M. Xiao, Electromagnetically induced Talbot effect, Appl. Phys. Lett. **98**, 081108 (2011).

[35] F. Wen, W. Wang, I. Ahmed, H. Wang, Y. Zhang, Y. Zhang, A. R. Mahesar, and M. Xiao, Two-dimensional Talbot self-imaging via Electromagnetically induced lattice, Sci. Rep. **7**, 41790 (2017).

[36] R. Bonifacio and L. De Salvo, Collective atomic recoil laser (CARL) optical gain without inversion by collective atomic recoil and self-bunching of two-level atoms, Nucl. Instrum. Methods Phys. Res., Sect. A **341**, 360 (1994).

[37] N. Piovella, R. Bonifacio, B. W. J. McNeil, and G. R. M. Robbb, Superradiant light scattering and grating formation in cold atomic vapours, Opt. Commun. **187**, 165 (2001).

[38] M. G. Moore and P. Meystre, Effects of atomic diffraction on the collective atomic recoil laser, Phys. Rev. A **58**, 3248 (1998).

[39] O. Zobay and G. M. Nikolopoulos, Dynamics of matter-wave and optical fields in superradiant scattering from Bose-Einstein condensates, Phys. Rev. A **72**, 041604(R) (2005).

[40] O. Zobay and G. M. Nikolopoulos, Spatial effects in superradiant Rayleigh scattering from Bose-Einstein condensates, Phys. Rev. A **73**, 013620 (2006).

[41] A. Hilliard, F. Kaminski, R. le Targat, C. Olausson, E. S. Polzik, and J. H. Müller, Rayleigh superradiance and dynamic Bragg gratings in an end-pumped Bose-Einstein condensate, Phys. Rev. A **78**, 051403(R) (2008).

[42] A. Schilke, C. Zimmermann, P. W. Courteille, and W. Guerin, Photonic Band Gaps in One-Dimensionally Ordered Cold Atomic Vapors, Phys. Rev. Lett. **106**, 223903 (2011).

[43] N. Ba, X. Zhong, L. Wang, J. Fei, Y. Zhang, Q. Bao, and L. Xiao, Tunable photonic band gaps and optical nonreciprocity by an RF-driving ladder-type system in moving optical lattice, Opt. Commun. **410**, 916 (2018).

[44] H. Yang, T. Zhang, Y. Zhang, and J. Wu, Dynamically tunable three-color reflections immune to disorder in optical lattices with trapped cold ^{87}Rb atoms, Phys. Rev. A **101**, 053856 (2020).

[45] K. S. Nawaz, L. Chen, C. Mi, Z. Meng, L. Huang, P. Wang, and J. Zhang, Photoassociation spectroscopy of weakly bound $^{87}Rb_2$ molecules near the $5P_{1/2} + 5S_{1/2}$ threshold by optical Bragg scattering in Bose-Einstein condensates, Phys. Rev. A **102**, 053326 (2020).

[46] S. Karpov and S. Stolyarov, Propagation and transformation of electromagnetic waves in one-dimensional periodic structures, Phys.-Usp. **36**, 1 (1993).

[47] S. Stringari and L. Pitaevskii, *Bose-Einstein Condensation*, (Oxford University Press, New York, 2003).

[48] S. Ostermann, F. Piazza, and H. Ritsch, Spontaneous Crystallization of Light and Ultracold Atoms, Phys. Rev. X **6**, 021026 (2016).

[49] O. Morice, Y. Castin, and J. Dalibard, Refractive index of a dilute Bose gas, Phys. Rev. A **51**, 3896 (1995).

[50] M. Gustavsson, E. Haller, M. J. Mark, J. G. Danzl, G. Rojas-Kopeinig, and H.-C. Nägerl, Control of Interaction-Induced Dephasing of Bloch Oscillations, Phys. Rev. Lett. **100**, 080404 (2008).

[51] K. Li, L. Deng, E. W. Hagley, M. G. Payne, and M. S. Zhan, Matter-Wave Self-Imaging by Atomic Center-of-Mass Motion Induced Interference, Phys. Rev. Lett. **101**, 250401 (2008).

[52] W. P. Lu, Y. K. Zhao, and P. F. Barker, Cooling molecules in optical cavities, Phys. Rev. A **76**, 013417 (2007).

[53] Y. K. Zhao, W. P. Lu, P. F. Barker, and G. J. Dong, Self-organisation and cooling of a large ensemble of particles in optical cavities, Faraday Discuss. **142**, 311 (2009).

[54] J. K. Asbóth, P. Domokos, H. Ritsch, and A. Vukics, Self-organization of atoms in a cavity field: Threshold, bistability, and scaling laws, Phys. Rev. A **72**, 053417 (2005).

[55] S. Slama, S. Bux, G. Krenz, C. Zimmermann, and P. W. Courteille, Superradiant Rayleigh Scattering and Collective Atomic Recoil Lasing in a Ring Cavity, Phys. Rev. Lett. **98**, 053603 (2007).